AIAA JOURNAL
Vol. 30, No. 9, September 1992

Stretching of Freestream Turbulence in the Stagnation Region

Chin Yi Wei* and Jiun Jih Miau†
National Cheng Kung University, Tainan, Taiwan 70101, Republic of China

Characteristics of stretched vortices in the stagnation region, due to the presence of freestream turbulence in the incident stream, were studied by means of spatial correlation. The spanwise length scale of the stretched vortices, l_m, and the characteristic height corresponding to the distance between the averaged position of the centers of the stretched vortices and the plate, H_v, are successfully correlated with the integral length scale of freestream turbulence. It is found that for each of the cases studied l_m and H_v are comparable, and l_m falls in the range of ~ 0.61–0.81 times the integral length scale of the corresponding freestream turbulence. Thus, the mechanism of inviscid vorticity stretching is suggested responsible for the development of three-dimensional vortical structures in the stagnation region outside the viscous layer.

Introduction

FOR flow past a bluff body, turbulent eddies embedded in the freestream are subject to stretching in the divergent stream near the forward stagnation point; thus, organized vortical structures may develop. As pointed out by several investigators,[1-4] these vortical structures play an important role influencing the fluid dynamic aspects and heat transfer characteristics of flow in the stagnation region. Examples are given for the heat transfer rate of heat exchangers,[1] the development of a turbulent boundary layer under the interaction of the oncoming disturbance amplified in the stagnation region and the stagnation laminar boundary layer,[2] and the enhancement of the heat transfer rate by the introduction of turbulence upstream of the stagnation region.[3,4]

Numerically, the effects of freestream turbulence on heat and momentum transfer in the stagnation region were studied by Traci and Wilcox,[5] Strahle et al.,[6] and Taulbee and Tran[7] with turbulence models. Although the heat transfer and momentum transfer in the stagnation region were predicted with a great success, the characteristics of flow structures formed in the stagnation region were not considered explicitly in these analyses.[5-7]

As learned from previous studies, the disturbances amplified in the stagnation region are selective.[2] Hodson and Nagib[8] studied the disturbances generated by a circular cylinder to be impinged on the two-dimensional bluff body and indicated the existence of a threshold condition corresponding to the incipient formation of the vortices in the stagnation region. Sadeh et al.[9,10] used theoretical analysis and experimental results, respectively, to explain the amplification of disturbances convecting toward the stagnation region. They found that, if the characteristic length scale of the disturbance is greater than a viscous length scale, λ_0, where $\lambda_0 = 2\pi/\sqrt{(a/\nu)}$ (a is the Hiemenz's constant and ν represents the kinematic viscosity of the fluid), the disturbance is amplified in the stagnation region. On the other hand, if the characteristic length scale of the disturbance is smaller than λ_0, the viscous dissipation effect dominates over the vortex stretching mechanism and the disturbance is damped as the flow approaches the stagnation region.

Hunt[11] proposed a view based on the rapid-distortion theory which assumes that the time taken for turbulence eddies distorted by the mean-flow straining effect as they pass the stagnation zone is much less than that required for turbulence eddies to change their own fluid dynamic properties resulting from viscous and nonlinear inertial forces. Thus, the viscous effect and the interaction between turbulence eddies are ignored. For a turbulent flow over a bluff body, the turbulence intensity will be amplified in the stagnation region if the characteristic length scale of the freestream turbulence, L_x, is much smaller than the characteristic dimension of the bluff body, W_d; namely, the mechanism of vorticity stretching is dominant, whereas the turbulence intensity is damped in the stagnation region if $L_x \gg W_d$. In this case the turbulent fluctuations act as an unsteady mean flow varying in magnitude and direction to the bluff body.[12] Theoretical predictions of Hunt[11] are confirmed by the experimental results of Bearman[13] and Britter et al.[14]

In explaining the phenomenon of vortical structures developed in the stagnation region, attempts from the viewpoint of flow instability were made by Kestin and Wood,[15] Wilson and Gladwell,[16] Stuart,[17] and Lyell and Huerre.[18] According to Wilson and Gladwell,[16] the three-dimensional disturbance of Gorlter type was found to be linearly stable in a two-dimensional stagnation flow. Stuart[17] imposed disturbance with no spanwise component of vorticity upstream of the stagnation region and indicated that freestream vorticity fluctuations can be received and accommodated by the stagnation boundary layer. Lyell and Huerre[18] indicated that the stagnation flow could be nonlinearly unstable if the initial disturbance level was higher than a critical amplitude. A marked difference noted between the approach of flow instability and the concept of vorticity stretching mentioned in the foregoing paragraph is that, in the stability analysis, one of the boundary conditions imposed forces the disturbance to be exponentially decaying far upstream of the stagnation region, whereas the concept of vorticity stretching infers that the vortical structures developed in the stagnation region are evolved from the freestream turbulence. Morkovin[19] made a comprehensive review on the theoretical studies and the experimental evidence relevant to this flow phenomenon and discussed whether the disturbances developed in the stagnation region are due to the mechanism of hydrodynamic instabilities is subject to further clarification.

In the present study the characteristics of the stretched vortical structures in the stagnation region are studied and are correlated with the freestream turbulence generated by different screens upstream of a bluff body. The purpose is to verify the linkage between the freestream conditions and the flow behavior observed in the stagnation region.

Experimental Setup

Experiments were conducted in a close-return low-speed wind tunnel with a test cross section of 280 × 450 mm. The

Received Aug. 19, 1991; revision received Jan. 17, 1992; accepted for publication Jan. 18, 1992.

*Graduate Student, Institute of Aeronautics and Astronautics.
†Professor, Institute of Aeronautics and Astronautics.

freestream turbulence intensity was ~0.3% in the absence of the bluff body and the turbulence generating screen. A flat plate of 50 mm in width, W_d, and 280 mm in length was placed normal to the flow to produce the desirable stagnation flowfield. This plate spanned the walls of the test section and was fitted by a two-dimensional profiled afterbody of 60 mm at its maximum width. The length of this afterbody was $4W_d$, which was designed to suppress vortex shedding downstream of the bluff body, therefore suppressing the irrotational velocity fluctuation induced by the wake in the forward stagnation region.[20] The coordinate system and the configuration of the two-dimensional bluff body are shown in Fig. 1. In addition, a cylinder of 50 mm in diameter fitted by the aforementioned afterbody was adopted for flow visualization study. Smoke-wire flow visualization experiments were conducted at U_0 = 1.5–4.2 m/s, where U_0 denotes the mean velocity of the incident flow. Hot-wire velocity measurements were performed at U_0 = 3.1–15.0 m/s for the cases with the flat normal plate.

Freestream conditions were controlled by three kinds of screens, denoted as S_I, S_{II}, and S_{III}. Both S_I and S_{II} were square-mesh woven screens with wire diameters of 0.8 and 2.4 mm, respectively, denoted d. The mesh sizes of S_I and S_{II} were 12.7 and 30.0 mm, respectively, corresponding to open area ratios of 0.88 and 0.85. The Reynolds numbers Re_d, based on the diameter of the wires of the screens, ranged from 165 to 800 and from 496 to 2400 for S_I and S_{II}, respectively. The screen S_{III} was made with strips of tapes 12.5 mm in width taped over a plastic diamond-shape mesh screen that had a mesh size of 11.5 mm and the diameter of the wires of the screen was 0.9 mm, shown in Fig. 2. The corresponding open area ratio was 0.52. This screen can produce turbulence whose intensity and characteristic length scale are much larger than those by S_I and S_{II}.

Hot-wire anemometers, DANTEC 55M01, with boundary-layer-type hot-wire probes, were employed for velocity measurement. As shown in Fig. 3a, if the measured position was located far upstream of the normal plate, the hot-wire probes were oriented to minimize the effect due to the disturbances caused by the probe support. If the measured position was near the wall, the hot-wire probes were rotated by 180 deg to measure the instantaneous velocity in the region very close to the wall (see Fig. 3b). It is realized that in the neighborhood of

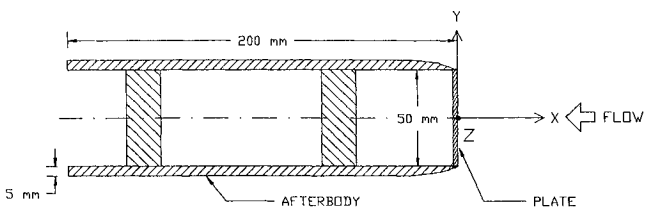

Fig. 1 Schematic view of the two-dimensional bluff body and the coordinate system employed.

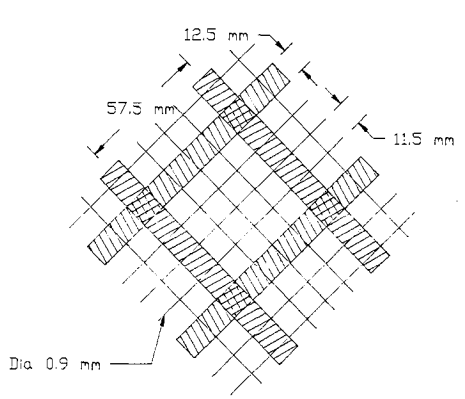

Fig. 2 Sketch of the screen S_{III}.

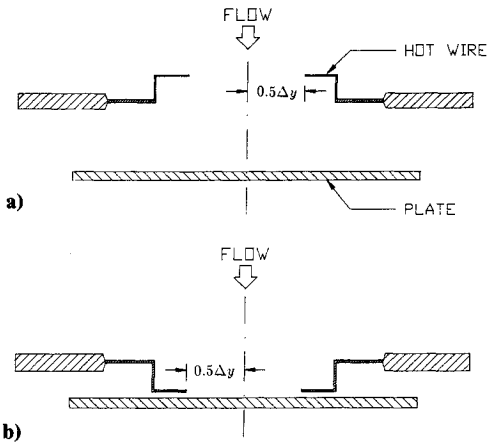

Fig. 3 Arrangement of the boundary-layer type hot-wire probes for the spatial correlation measurement: a) far upstream of the wall; and b) near the wall.

Table 1 Freestream turbulence intensities for arrangements I–IV at U_0 = 3.1 and 9.6 m/s.

Arrangement	U_0, m/s	$\frac{\overline{u^2}^{1/2}}{U_0}$, %	$\frac{\overline{v^2}^{1/2}}{U_0}$, %	$\frac{\overline{w^2}^{1/2}}{U_0}$, %
I	3.1	1.3	1.1	1.1
I	9.6	1.3	1.1	1.1
II	3.1	2.7	2.2	2.2
II	9.6	2.8	2.2	2.2
III	3.1	7.4	6.3	6.1
III	9.6	8.0	7.3	7.1
IV	3.1	1.8	1.5	1.5
IV	9.6	1.9	1.7	1.7

the stagnation point reversed flow is possible because of the formation of stretched vortices. This region was regarded as unsuitable for hot-wire measurement.

Since a single-wire probe senses all of the velocity components perpendicular to the wire, in a divergent stream of the stagnation region the direction corresponding to the instantaneous velocity fluctuation measured by a boundary-layer probe is not determinable. Nevertheless, in the present study our interest is primarily on the spatial coherency of turbulence eddies as they convect toward the stagnation region; hence, the instantaneous velocity fluctuations measured can be utilized for representing the signatures of the eddies, which are subsequently employed for cross-correlation calculations. The space-time correlation is defined by

$$R_{s_A s_B}(\Delta x, \Delta y, \Delta z, \Delta t) = \frac{\overline{s_A(X_A, Y_A, Z_A, t_0) s_B(X_B, Y_B, Z_B, t)}}{\sqrt{\overline{s_A^2}}\sqrt{\overline{s_B^2}}} \quad (1)$$

where s_A and s_B denote the fluctuating quantities measured at positions A and B, respectively; the spatial separation of the two probes is defined by $\Delta x = X_B - X_A$, $\Delta y = Y_B - Y_A$, and $\Delta z = Z_B - Z_A$; Δt denotes the time delay between the two signals measured; and the overbar represents the time average. It should be noted that the measuring positions A and B are not shown explicitly in the expression of $R_{s_A s_B}$ on the left-hand side of Eq. (1). To avoid the confusion, in the presentation of the correlation results given later, the measuring positions will be described along with the data.

In the experiment the normal plate was situated 62 cm downstream of one of the screens S_I, S_{II}, or S_{III} or 40 cm downstream of the screen S_I. Hereafter, these experimental arrangements are referred to as I, II, III, and IV, respectively. The turbulence intensities measured by a X-type hot wire at the location of the normal plate with respect to these four arrangements, while the plate was absent from the flowfield,

Table 2 Relation between the longitudinal integral length scale of freestream turbulence and the spanwise length scale of the counter-rotating vortices

Arrangement	Re_{W_d}	L_x, mm	l_m, mm	l_m/L_x
I	10,000	7.42	5.62	0.76
I	16,600	7.36	4.63	0.63
I	25,000	6.54	4.38	0.67
I	32,000	6.11	4.39	0.72
I	50,000	5.53	3.68	0.67
II	10,000	9.18	6.45	0.70
II	16,600	9.36	6.12	0.65
II	25,000	9.64	6.37	0.66
II	32,000	9.78	6.17	0.63
II	50,000	9.82	6.41	0.65
III	10,000	21.16	16.65	0.79
III	16,600	21.96	16.76	0.76
III	25,000	20.60	16.11	0.78
III	32,000	20.43	13.38	0.65
IV	10,000	5.94	4.78	0.80
IV	16,600	5.45	4.38	0.80
IV	25,000	5.17	3.97	0.77
IV	32,000	5.17	3.90	0.75
IV	50,000	5.23	3.88	0.74

95% confidence interval of l_m/L_x is ~ 0.1 for each case.

are listed in Table 1. The spatial nonuniformities of the streamwise mean velocity distribution measured for arrangements I and IV are $<1\%$; this uniformity is $<2\%$ for arrangement II and $<5\%$ for arrangement III. Furthermore, a reference integral length scale, L_x, is defined which corresponds to the longitudinal integral length scale of the turbulent flow measured at the location of the plate, in the absence of the plate. The values of L_x obtained with respect to the experimental arrangements at a number of Reynolds numbers studied are listed in Table 2. The expense for obtaining large integral length scale of freestream turbulence for arrangement III is the increase of turbulence intensity and spatial nonuniformity in velocity distribution.

The values of L_x corresponding to all the cases listed in Table 2 largely fall in the range that satisfies the criteria of vorticity amplification suggested by the rapid distortion theory[11,13,14] and by the vorticity amplification theory[2,9,10] ($\lambda_0 < L_x \ll W_d$). For example, at $U_0 = 5.0$ m/s ($R_{e_{wd}} = 16{,}600$) the viscous length scale, $\lambda_0 \approx 2.3$ mm, is smaller than the values of L_x for arrangements I–IV shown in Table 2. On the other hand, the ratios of L_x/W_d, which were 0.147, 0.187, and 0.109 at $U_0 = 5.0$ m/s for arrangements I, II, and IV, respectively, satisfy the criterion of $L_x/W_d \ll 1$. For arrangement III the ratio of L_x/W_d is 0.439, which should not be regarded as very small compared to 1. Consequently, the obtained results of this case indicate much weaker effect of vortex stretching in the stagnation region than those seen in the other cases (see Figs. 6 and 7 given later).

Figure 4 shows the spanwise correlation distributions of $R_{u_A u_B}(0, 0, \Delta z, 0)$ for arrangements I and II at the cross-sectional plane of $X = 0$ at $U_0 = 3.1$ and 9.6 m/s while the normal plate is absent. The symbols u_A and u_B denote the streamwise velocity fluctuations measured at positions A and B, respectively, and Δz denotes the spanwise separation between the positions A and B. In the figure the vertical line plotted with each of the data points indicates the bandwidth of the 95% confidence interval associated with the mean value obtained. As Δz increases the correlation values decrease to zero without going negative substantially. This tendency coincides with the characteristic of isotropic turbulence,[21] implying that the turbulent flows produced with respect to arrangements I and II at $X = 0$, in the absence of the bluff body, approach the isotropic condition.

When the bluff body is present in the flow, it is found that the distributions of the streamwise mean velocity measured along the mean stagnation streamline outside the viscous region for arrangements I–IV, at a fixed freestream velocity, appear to be identical (see Fig. 5). This implies that the distribution of the mean stagnation flow measured is not affected by the turbulence intensity, which confirms the statements made by Traci and Wilcox[5] and Taulbee and Tran.[7] In the present experiments the nondimensional values of aW_d/U_0 for the cases of U_0 from 3.1 to 9.6 m/s are ~ 1.1. As noted in Fig. 5, the region in which the streamwise velocity varies linearly with respect to X is found at $X < 0.5W_d$.

Physical Considerations of Vorticity Amplification

Based on an assumption that the mean stagnation flow outside of the boundary-layer region is irrotational, the vorticity equation can be given as

$$\frac{D\omega_i}{Dt} = \omega_j \frac{\partial U_i}{\partial X_j} + \omega_j \frac{\partial u_i}{\partial X_j} + \nu \frac{\partial^2 \omega_i}{\partial X_j^2} \tag{2}$$

where ω_i indicates the fluctuating vorticity in connection with the freestream turbulence, and U_i and u_i designate the mean and fluctuating velocities, respectively. Here, $i, j = 1, 2$, and 3 are the tensorial notations. The equivalence between the tensorial symbols and the symbols appearing in the context should

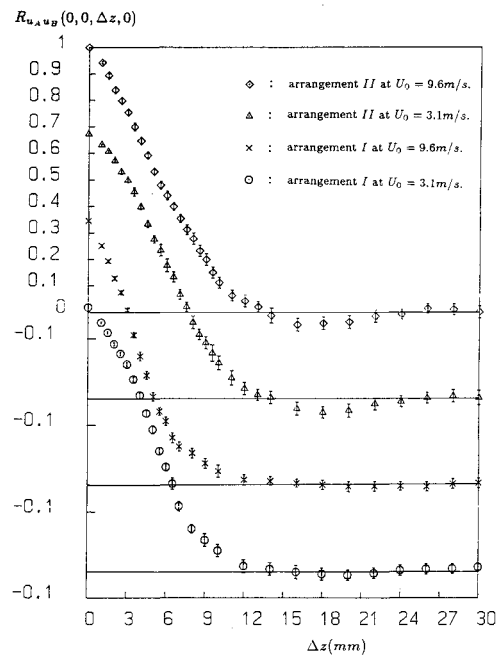

Fig. 4 Distributions of $R_{u_A u_B}(0, 0, \Delta z, 0)$ for arrangements I and II, without the presence of the bluff body.

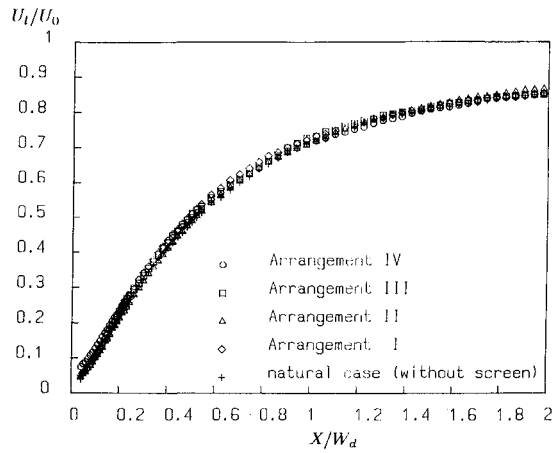

Fig. 5 Distributions of mean streamwise velocity along the mean stagnation streamline for the cases studied at $U_0 = 5.0$ m/s.

be noted that $(X_1, X_2, X_3) = (X, Y, Z)$, $(\omega_1, \omega_2, \omega_3) = (\omega_x, \omega_y, \omega_z)$, $(U_1, U_2, U_3) = (U, V, W)$, and $(u_1, u_2, u_3) = (u, v, w)$. It is argued from the assumption of the rapid-distortion theory that the second and third terms on the right-hand side of Eq. (2) are small compared to the first term; thus, the vorticity equation can be simplified as[11]

$$\frac{D\omega_i}{Dt} = \omega_j \frac{\partial U_i}{\partial X_j} \tag{3}$$

This equation implies that the development of oncoming disturbance is controlled by the mechanisms of vortex stretching and tilting in the stagnation region. If one substitutes the potential flow distribution, $U = -aX$ and $V = aY$, into Eq. (3), one obtains

$$\frac{1}{\omega_x}\frac{D\omega_x}{Dt} = -a \tag{4}$$

and

$$\frac{1}{\omega_y}\frac{D\omega_y}{Dt} = a \tag{5}$$

Equations (4) and (5) exhibit that, as far as the action of the mean flow is concerned, the mechanism of vortex stretching plays the vital role on the dynamics of vorticity of the oncoming turbulence while the mechanism of vortex tilting is not important.

Physically speaking, since the fluctuating vorticity associated with freestream turbulence is unsteady, the nonstationary behavior of the stretched vortices developed in the stagnation region is also expected. This character is evidenced by comparing two smoke-wire visualization photographs shown in Fig. 6 that were taken at arbitrary time instants, at $U_0 = 2.0$ m/s, for arrangement I. The Reynolds number based on the diameter of the smoke wire is 0.4 mm, and the local mean velocity is ~ 33. Thus, the effect due to the presence of the smoke wire is regarded to be insignificant.[22] As revealed from the photographs, the stretched vortices near the wall are developed into a basically counter-rotating form that resembles the sketches provided by Kestin and Wood[15] and Lyell and Huerre[18] deduced from the theoretical predictions.

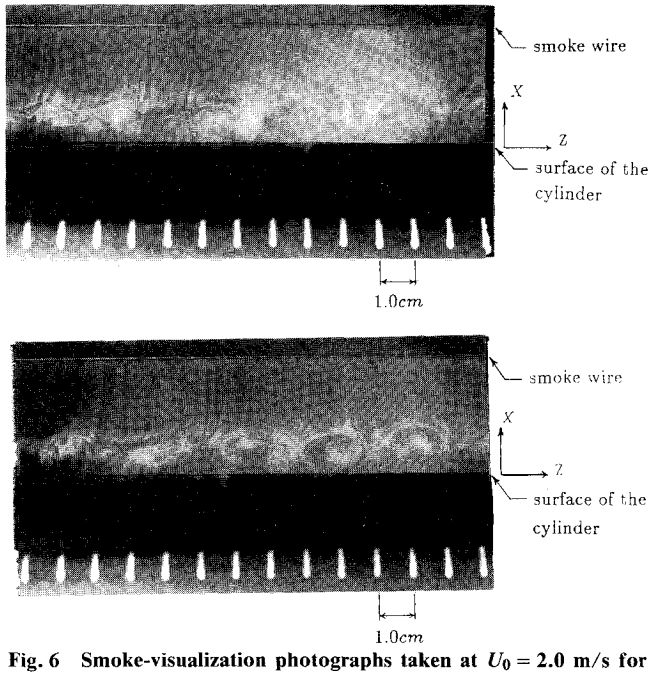

Fig. 6 Smoke-visualization photographs taken at $U_0 = 2.0$ m/s for arrangement I, for a cylinder of 50 mm diameter fitted with the profiled afterbody.

Results and Discussion

Stretching of Oncoming Vorticity Filaments

Stretching of the freestream turbulence as flow approaches the stagnation region can be illustrated by isovalue contours of $R_{q_A q_B}(0, \Delta y, 0, 0)$ shown in Fig. 7, where q_A and q_B denote the velocity fluctuations measured by two boundary-layer probes with the hot wires aligned in Z direction at positions A and B, respectively. The measurements were performed in the cross-sectional planes from $X = 1$ to 50 mm, whereas, in each of the cross-sectional planes measured, the separation between the two hot-wire probes varies from $\Delta y = 2$ to 44 mm. The two hot-wire probes were situated symmetrically with respect to $Y = 0$, fixed at $Z = 0$. The isovalue contours in Fig. 7 are plotted in a coordinate system in which the horizontal axis indicates half the separation distance between the two hot wires, $\frac{1}{2}\Delta y$, and the vertical axis indicates the location of the cross-sectional plane measured. The contour diagram in each of the plots is constructed from a set of data obtained over 150 grid points in the flowfield. The value of $R_{q_A q_B}(0, \Delta y, 0, 0)$ at each point was reduced from 25 sets of velocity correlation measurements through an ensemble-averaging procedure. The region around the origin, indicated by the hatch lines in each of the five plots in Fig. 7, signifies the occurrence of flow reversal observed.

According to the isovalue contours shown in each of the plots of Fig. 7, one can identify a cross-sectional plane of constant X where the turbulence eddies are stretched to an ultimate situation. This X location can be considered as the averaged position of the centers of the stretched vortices developed in the stagnation region (see also the flow visualization photographs in Fig. 6). The distance between this cross-sectional plane and the surface of the normal plate is denoted as H_v and characterizes the average size of the stretched vortices.

The values of H_v corresponding to the arrangements I, II, and III, at $U_0 = 3.1$ m/s, shown in Figs. 7a, 7b, and 7c are approximately 5.0, 6.2, and 12.9 mm, respectively. The values of H_v corresponding to the arrangements I and II, at $U_0 = 9.6$ m/s, shown in Figs. 7d and 7e, are 3.6 and 5.8 mm, respectively. On the other hand, regarding the Hiemenz similarity solution, the thickness of a two-dimensional stagnation boundary layer is estimated to be ~ 1.1 mm at $U_0 = 3.1$ m/s or ~ 0.64 mm at $U_0 = 9.6$ m/s. Hence, a comparison of the physical lengths given previously indicates that the values of H_v found are much larger than the stagnation boundary-layer thickness estimated. This finding agrees with the flow visualization results of Sadeh and Brauer[2] that the vortices developed from the wakes behind the cylindrical rods upstream were stretched and situated primarily outside the stagnation boundary layer.

A feature obtained from Fig. 7 is that the values of H_v vary with the flow conditions studied. However, the ratios H_v/L_x are found to be about 0.68, 0.66, and 0.61 with respect to arrangements I, II, and III at $U_0 = 3.1$ m/s, and are 0.59 and 0.59 with respect to arrangements I and II at $U_0 = 9.6$ m/s. Consequently, the nondimensional ratios H_v/L_x corresponding to these flow conditions are comparable, which strongly suggests that the characteristic size of the stretched vortices in the stagnation region is controlled by the oncoming turbulence. As noted, at $U_0 = 3.1$ m/s the ratio H_v/L_x for arrangement III (Fig. 7c) deviates somewhat from the ratios for arrangements I and II. Following the argument of Hunt,[11] this is attributed to the fact that the characteristic scale of freestream turbulence of arrangement III is not very small compared to the characteristic dimension of the plate.

As noted in the preceding paragraph, the ratios H_v/L_x of arrangements I and II decrease slightly as the Reynolds numbers increase, which suggests that Reynolds number is an influential parameter. This could be due to the presence of the viscous layer on the wall that affects the development of stretched vortices. A study of the viscous effect of the present flow is beyond the scope of this work; this topic will be pursued in the future.

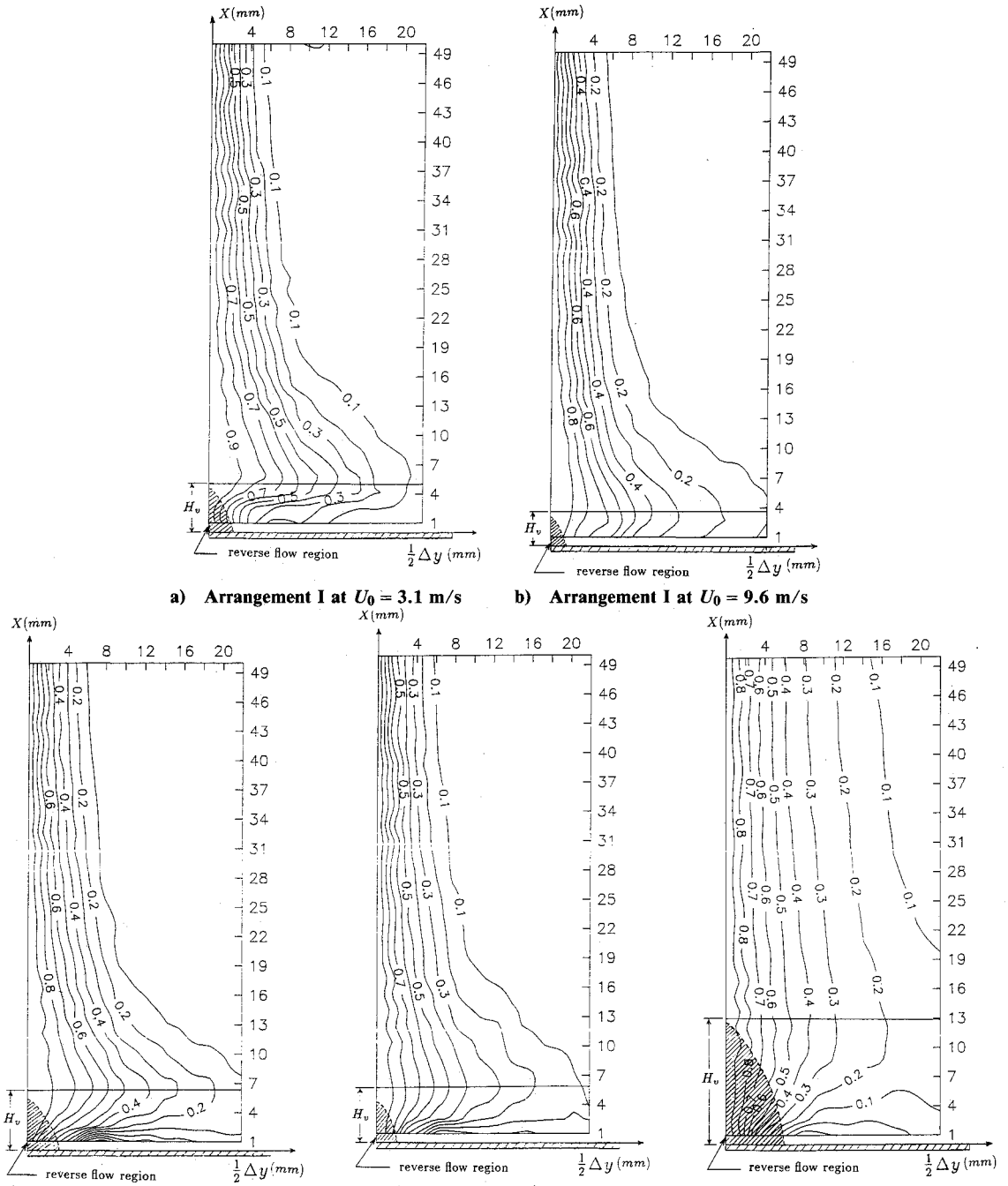

a) Arrangement I at $U_0 = 3.1$ m/s b) Arrangement I at $U_0 = 9.6$ m/s

c) Arrangement II at $U_0 = 3.1$ m/s d) Arrangement II at $U_0 = 9.6$ m/s e) Arrangement III at $U_0 = 3.1$ m/s

Fig. 7 Isovalue contours of $R_{q_A q_B}(0, 0, \Delta z, 0)$.

Further Analysis on the Effect of Vorticity Amplification

One considers a simplified situation in which a turbulence eddy is modeled by a cross-streamwise vortex tube aligned in the Y direction and this vortex tube is convecting toward the stagnation region. It is assumed that the eddy has uniform vorticity ω_y distributed in a cross-sectional area A. By the inviscid assumption relevant to the flow outside the viscous layer, the total vorticity flux is conserved; i.e.,

$$\frac{\mathrm{D}\omega_y A}{\mathrm{D}t} = 0 \tag{6}$$

where D/Dt denotes the substantial derivative. On the other hand, since the present flow is assumed to be incompressible, the physical volume of the eddy remains unchanged:

$$\frac{\mathrm{D}AL}{\mathrm{D}t} = 0 \tag{7}$$

where L represents a characteristic length scale of the eddy in the Y direction. Equations (6) and (7) result in

$$\frac{1}{\omega_y}\frac{\mathrm{D}\omega_y}{\mathrm{D}t} = \frac{1}{L}\frac{\mathrm{D}L}{\mathrm{D}t} \tag{8}$$

The term on the right-hand side of Eq. (8) represents the strain rate of the eddy in the Y direction; i.e.,

$$\frac{1}{L}\frac{\mathrm{D}L}{\mathrm{D}t} = \frac{\partial V}{\partial Y} \tag{9}$$

Note that substituting the expression of Eq. (9) into Eq. (8) recovers the inviscid vorticity equation [see Eq. (3)]. For $V = aY$, an integration following the streamline in the stagnation region gives

$$\frac{L}{L_0} = e^{at} \tag{10}$$

where t indicates the time associated with convection of the eddy and L_0 is the length of the eddy at $t = 0$. By the Lagrangian approach given earlier, it can also be shown that

$$\frac{X}{X_0} = e^{-at} \tag{11}$$

where X_0 is the location of the eddy at $t = 0$. Since the fluid parcel follows the mean flow in the divergent stream of the stagnation region, Eqs. (8), (10), and (11) can be combined as

$$\frac{\omega_y}{\omega_{y_0}} = \frac{L}{L_0} = \frac{X_0}{X} \tag{12}$$

where ω_{y_0} denotes the initial vorticity of the eddy at $t = 0$. Equation (12) shows that, because of the effect of vorticity stretching in the stagnation region, the cross-streamwise length of the eddy is inversely proportional to the distance from the normal surface, and vorticity change can be estimated by the variation of the length of the eddy in the Y direction.

Assuming that Eq. (12) may also describe the statistical behavior of turbulent eddies evolving along the mean stagnation streamline, one therefore makes a comparison of the stretching effect estimated by Eq. (12) with that reduced from the experimental data shown in Fig. 7. This comparison is given in Table 3. In this table L is chosen to be the separation distance between the two hot-wire probes, Δy, for which $R_{q_A q_B}(0, \Delta y, 0, 0) = 0.6$. Figure 7 shows that, at the cross-sectional plane $X \approx H_v$, the distribution of $R_{q_A q_B}(0, \Delta y, 0, 0)$ vs $\frac{1}{2}\Delta y$ has the steepest gradient around $R_{q_A q_B}(0, \Delta y, 0, 0) = 0.6$; thus, the characteristic length of turbulence eddies, L, can be represented by the corresponding separation distance for minimizing the uncertainty in length measurement. In Table 3 the location of X_0 is taken to be $0.5W_d$. Note that the initial location of X_0 has to be chosen in the region where the streamwise velocity varies linearly along the mean stagnation streamline, to comply with the definition of the stagnation flow distribution. Table 3 indicates that the stretching effect estimated by Eq. (12), represented by the values of X_0/X, is

Table 3 Comparison of experimental and theoretical estimations on vortex stretching in the stagnation region

Arrangement	Re_{W_d}	$\frac{X_0}{X(X = H_v)}$	$\frac{L(X = H_v)}{L_0(X = 0.5W_d)}$
I	10,000	4.99	3.13
II	10,000	4.04	2.80
III	10,000	1.94	1.23
I	32,000	6.70	2.95
II	32,000	4.33	2.42

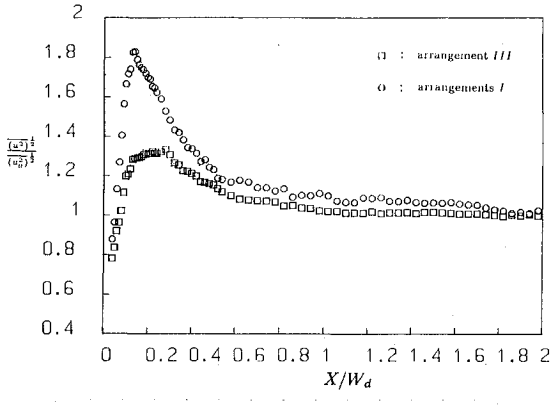

Fig. 8 Developments of the streamwise velocity fluctuation along the mean stagnation streamline for arrangements I and III at $U_0 = 5.0$ m/s.

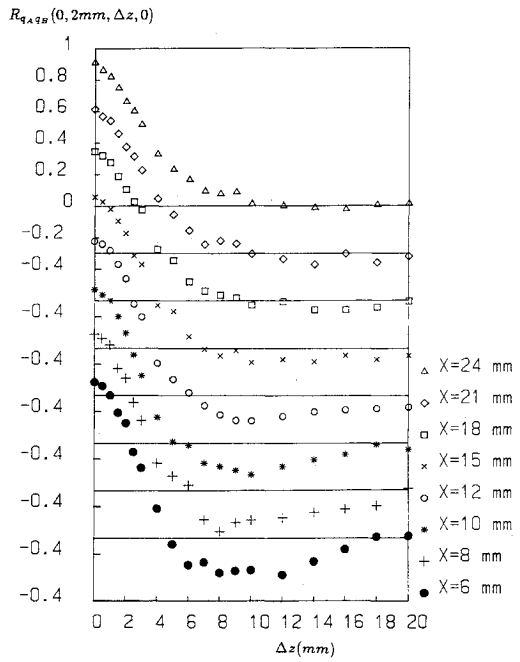

Fig. 9 Distributions of $R_{q_A q_B}(0, 2\text{ mm}, \Delta z, 0)$ at $X \approx H_v$ and farther upstream for arrangement I at $U_0 = 5.0$ m/s ($H_v \approx 5$ mm).

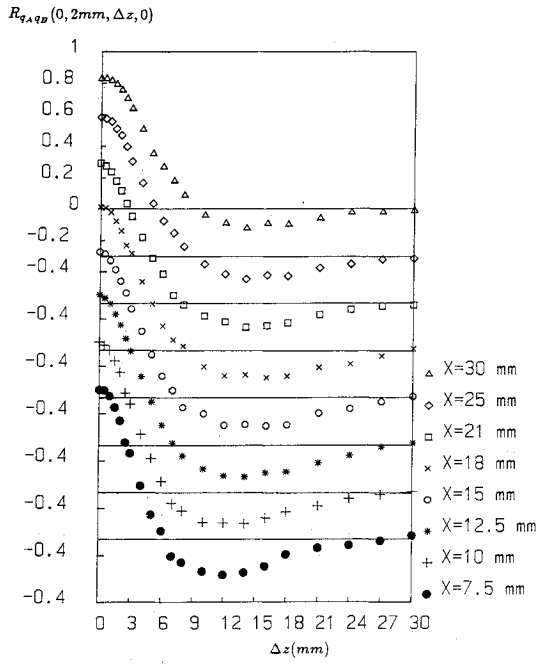

Fig. 10 Distributions of $R_{q_A q_B}(0, 2\text{ mm}, \Delta z, 0)$ at $X \approx H_v$ and farther upstream for arrangement II at $U_0 = 5.0$ m/s ($H_v \approx 6$ mm).

greater than the estimation deduced from Fig. 7, represented by the values of L/L_0, by a factor of 2 roughly. Although the trends of the theoretical estimation and the experimental results obtained are similar qualitatively, the discrepancy is significant. On the other hand, it is estimated from the experimental data obtained that in the region of $H_v < X < W_d$ the turbulence interaction effect and the viscous diffusion effect [i.e., the second and third terms on the right-hand side of Eq. (2)], are negligible compared to the mean flow stretching effect. Thus, this discrepancy could result because the stagnation flow distribution assumed for deriving Eq. (12) is in effect valid in the vicinity of the stagnation streamline; thus, the stretching effect should become less pronounced farther away from the stagnation streamline.

As shown in Table 3, the case of least stretching is due to arrangement III, since for this case the turbulence integral

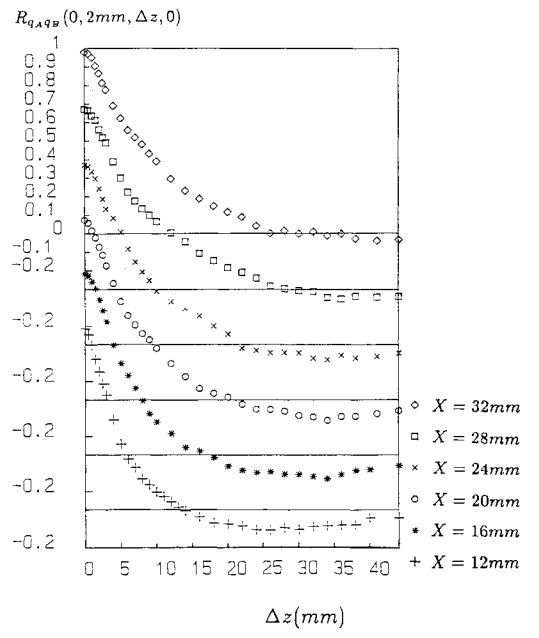

Fig. 11 Distributions of $R_{q_Aq_B}$(0, 2 mm, Δz, 0) at $X \approx H_v$ and farther upstream for arrangement III at $U_0 = 5.0$ m/s ($H_v \approx 12$ mm).

length scale of L_x produced is the largest among all the cases listed. This can also be seen from a comparison of the developments of the turbulence intensity, $\overline{u^2}^{1/2}/u_0^{2\,1/2}$, obtained along the mean stagnation streamline with respect to the arrangements I and III (see Fig. 8). Here, u and u_0 denote the local and reference streamwise velocity fluctuations, respectively, where u_0 is obtained at $X = 0$ in the absence of the bluff body. Figure 8 shows that for arrangement I the maximum value of $\overline{u^2}^{1/2}/u_0^{2\,1/2}$ obtained is >1.8, whereas for arrangement III the maximum value of $\overline{u^2}^{1/2}/u_0^{2\,1/2}$ obtained is <1.4. It is noted that the streamwise locations corresponding to the maximum values of $\overline{u^2}^{1/2}/u_0^{2\,1/2}$ shown in these two plots roughly coincide to the cross-sectional planes of $X = H_v$.

Spanwise Correlation Distributions at Different Cross-Sectional Planes

Figures 9, 10, and 11 show the distributions of spatial correlation coefficients, $R_{q_Aq_B}$ (0, 2 mm, Δz, 0), obtained in the cross-sectional planes of constant X for arrangements I, II, and III, respectively, at $U_0 = 5.0$ m/s. In each of the cross-sectional planes measured the two hot-wire probes were situated at $Y = \pm 1$ mm, respectively (i.e., $\Delta y = 2$ mm), and one of the hot-wire probes was fixed at the spanwise position, $Z = 0$, whereas the other was moved in a spanwise direction.

A feature that these figures have in common is that the distribution of $R_{q_Aq_B}$ (0, 2 mm, Δz, 0) obtained far upstream of the normal plate is similar to that obtained in the case without the presence of the bluff body shown in Fig. 4. However, as the measured cross-sectional plane gets closer to the normal plate, the distribution of $R_{q_Aq_B}$ (0, 2mm, Δz, 0) obtained appears to have a valley region in which the values measured are substantially negative. This appearance indicates that antiphase-like velocity fluctuations are pronounced for two hot wires situated with certain spanwise separations. Consequently, an implication of these observations is that turbulence eddies become more organized and orientated along the Y axis as they approach the normal plate. As shown in each of the figures, at the cross-sectional plane $X \approx H_v$, the spanwise separation corresponding to the most negative correlation value obtained is about twice that corresponding to the first zero interception of the curve on the horizontal axis. Thus, the spanwise separation of the two hot-wire probes corresponding to the first zero interception in the correlation curve measured at $X \approx H_v$, called l_m, is suggested to characterize the averaged spanwise dimension of the stretched vortices. The values of l_m obtained for the cases studied are listed in Table 2.

Table 2 indicates that the ratios l_m/L_x of all of the cases listed are generally fluctuating about the mean, 0.71. Furthermore, taking into account the fact that each of the values of l_m/L_x listed is associated with a 95% confidence interval of a bandwidth of ~ 0.1, one can say that the ratios of l_m/L_x shown in Table 2 largely fall in the range of 0.61–0.81. As a result, a strong correlation between the spanwise length scale of the stretched vortices in the stagnation region and the integral length scale of the freestream turbulence is realized. It should be noted that this consistency is held even for the cases with arrangement III, in which the freestream turbulence is considered to be far from isotropic.

It is interesting to note that the characteristic heights of the stretched vortices, H_v, shown in Fig. 7, are comparable to l_m listed in Table 2 under the same flow conditions. Physically, this infers that the stretched vortices developed in the stagnation region are essentially aligned in the Y direction. H_v or l_m simply represents the characteristic dimension of the cross-sectional area of the stretched vortices. Thus, downstream of the stagnation region these stretched vortices are basically in a form of counter-rotating streamwise vortices, whose cross-sectional views are exemplified in the photographs in Fig. 6.

It should be pointed out that the present work does not extend to the flow characteristics in the viscous layer of the stagnation region; therefore, the interaction between the stretched flow structures and flow in the region adjacent to the wall is not clarified. For instance, it is expected that the parameter of Reynolds number that does not appear in the nondimensional form of the length scale of the stretched vortical structures in the foregoing analysis may play an important role in the flow phenomena in the viscous region. Since for a number of engineering applications such as heat transfer prediction the flow characteristics in the viscous layer of the stagnation region are of greatest concern, it is deemed worthwhile to attempt some discussion in this respect based on the present results obtained. In predicting the heat transfer effect of a stagnation turbulent flow, Traci and Wilcox[5] suggested that the stagnation flowfield can be characterized into three regions, in which the wall region adjacent to the wall surface is assumed to have a thickness of $6\sqrt{\nu/a}$, equivalent to 2.5 times the thickness of the stagnation boundary layer according to the Hiemenz solution. At the edges of the wall region, $X = 6\sqrt{\nu/a}$, the flow is characterized by turbulence energy that reaches the maximum value. On the other hand, Fig. 8 indicates that the location corresponding to the maximum streamwise turbulence intensity measured along the mean stagnation streamline almost coincides with the location of $X \approx H_v$. The value of H_v is found to be ~ 5–10 times the boundary-layer thickness of the Hiemenz solution depending on the length scale of L_x of the oncoming turbulence. Hence, the preceding comparison suggests that the thickness of the wall region given in the computation model of Traci and Wilcox[5] could be further modified by taking the characteristics of the freestream turbulence into consideration.

Concluding Remarks

This work shows that imposed freestream turbulence leads to organized vortical structures developed in the stagnation region. By means of spatial correlation it is found that the characteristic scales of the stretched vortices developed in the stagnation region are well correlated with the integral scales of the oncoming turbulence. The spanwise length scale of the stretched vortices, l_m, can be normalized by the integral length scale of the grid-generated freestream turbulence to a nominal value between 0.61 and 0.81. Furthermore, the characteristic height H_v corresponding to the distance between the averaged position of the centers of stretched vortices and the normal plate surface is comparable to the spanwise length scale l_m of

the stretched vortices. This coincidence signifies that the stretched vortices developed in the stagnation region are aligned in the Y direction essentially, and l_m or H_v corresponds to the characteristic dimension of the cross-sectional area of the stretched vortices.

It is shown that vorticity stretching is initiated far upstream of the stagnation region, seen also from the inviscid vorticity equation, and the thickness of the stagnation boundary layer is much smaller than the averaged size of stretched vortices. Thus, the process of vorticity stretching in the stagnation region is suggested to be inviscid essentially. This gives a support to the viewpoints of Hunt[11] and Sadeh et al.[9,10]

Acknowledgment

This work was supported by National Science Council, Republic of China, under Contract NSC 80-0401-E006-35.

References

[1]Kestin, J., "The Effect of Free Stream Turbulence on Heat Transfer Rates," *Advances in Heat Transfer,* Vol. 3, 1966, pp. 1-32.

[2]Sadeh, W. Z., and Brauer, H. J., "A Visual Investigation of Turbulence in Stagnation Flow about a Circular Cylinder," *Journal of Fluid Mechanics,* Vol. 99, Pt. 1, 1980, pp. 53-64.

[3]Kestin, J., and Wood, R. T., "Enhancement of Stagnation-Line Heat Transfer by Turbulence," *Progress in Heat and Mass Transfer,* Vol. 2, 1969, pp. 249-253.

[4]Sutera, S. P., Maeder, P. F., and Kestin, J., "On the Sensitivity of Heat Transfer in the Stagnation-Point Boundary Layer to Free-Stream Vorticity," *Journal of Fluid Mechanics,* Vol. 16, 1963, pp. 497-520.

[5]Traci, R. M., and Wilcox, D. C., "Freestream Turbulence Effect on Stagnation Point Heat Transfer," *AIAA Journal,* Vol. 13, No. 7, 1975, pp. 890-896.

[6]Strahle, W. C., Sigman, R. K., and Meyer, W. L., "Stagnation Turbulent Flows," *AIAA Journal,* Vol. 25, No. 8, 1987, pp. 1071-1077.

[7]Taulbee, D. B., and Tran, L., "Stagnation Streamline Turbulence," *AIAA Journal,* Vol. 26, No. 8, 1988, pp. 1011-1013.

[8]Nagib, H. M., and Hodson, P. R., "Vortices Induced in a Stagnation Region by Wakes," *Aerodynamic Heating and Thermal Protection Systems,* edited by L. S. Fletcher, Vol. 59, Progress in Astronautics and Aeronautics, AIAA, New York, 1977, pp. 66-90.

[9]Sadeh, W. Z., Sutera, S. P., and Maeder, P. F., "Analysis of Vorticity Amplification in the Flow Approaching a Two-Dimensional Stagnation Point," *Zeitschrift fuer Angewandte Mathematik und Physik,* Vol. 21, 1970, pp. 669-716.

[10]Sadeh, W. Z., Sutera, S. P., and Maeder, P. F., "An Investigation of Vorticity Amplification in Stagnation Flow," *Zeitschrift fuer Angewandte Mathematik und Physik,* Vol. 21, 1970, pp. 717-742.

[11]Hunt, J. C. R., "A Theory of Turbulent Flow Around Two-Dimensional Bluff Bodies," *Journal of Fluid Mechanics,* Vol. 61, Pt. 4, 1973, pp. 625-706.

[12]Bearman, P. W., and Morel, T., "Effect of Free Stream Turbulence on the Flow around Bluff Bodies," *Progress in Aerospace Science,* Vol. 20, 1983, pp. 97-123.

[13]Bearman, P. W., "Some Measurements of the Distortion of Turbulence Approaching a Two-Dimensional Bluff Body," *Journal of Fluid Mechanics,* Vol. 53, Pt. 3, 1972, pp. 451-467.

[14]Britter, R. E., Hunt, J. C. R., and Mumford, J. C., "The Distortion of Turbulence by a Circular Cylinder," *Journal of Fluid Mechanics,* Vol. 92, Pt. 2, 1979, pp. 269-301.

[15]Kestin, J., and Wood, R. T., "On the Stability of Two-Dimensional Stagnation Flow," *Journal of Fluid Mechanics,* Vol. 44, Pt. 3, 1970, pp. 461-479.

[16]Wilson, D. R., and Gladwell, I., "The Stability of a Two-Dimensional Stagnation Flow to Three-Dimensional Disturbances," *Journal of Fluid Mechanics,* Vol. 84, Pt. 3, 1978, p. 517.

[17]Stuart, J. T., "Instability of Laminar Flows, Non-Linear Growth of Fluctuations, and Transition to Turbulence," *Turbulence and Chaotic Phenomena in Fluids, Proceedings IUTAM Conference,* edited by T. Tatsumi, Elsevier Publishing, Amsterdam, 1983, pp. 17-26.

[18]Lyell, M. J., and Huerre, P., "Linear and Nonlinear Stability of Plane Stagnation Flow," *Journal of Fluid Mechanics,* Vol. 161, 1985, pp. 295-312.

[19]Morkovin, M. V., "On the Question of Instability Upstream of Cylindrical Bodies," NASA CR 3231, Dec. 1979.

[20]Wei, C. Y., and Miau, J. J., "Influences of Freestream Turbulence and Wake on Flow near the Stagnation Region," *Journal of Chinese Society of Mechanical Engineering,* Vol. 12, No. 6, 1991, pp. 555-562.

[21]Hinze, J. O., *Turbulence,* 2nd ed., McGraw-Hill, 1975.

[22]Roshko, A., "On the Development of Turbulent Wakes from Vortex Streets," NACA Rept. 1911, 1953.